Appearance of objectivity for NV centers interacting with dynamically polarized nuclear environment

Kwiatkowski, Damian; Cywinski, Lukasz; Korbicz, Jarosaw K.

DOI
10.1088/1367-2630/abeffd

Publication date
2021

Document Version
Final published version

Published in
New Journal of Physics

New Journal of Physics
The open access journal at the forefront of physics

Deutsche Physikalische Gesellschaft DPG IOP Institute of Physics

PAPER • OPEN ACCESS

Appearance of objectivity for NV centers interacting with dynamically polarized nuclear environment

To cite this article: Damian Kwiatkowski *et al* 2021 *New J. Phys.* **23** 043036

New Journal of Physics
The open access journal at the forefront of physics

Deutsche Physikalische Gesellschaft DPG
IOP Institute of Physics

Published in partnership with: Deutsche Physikalische Gesellschaft and the Institute of Physics

OPEN ACCESS

RECEIVED
23 December 2020

REVISED
16 March 2021

ACCEPTED FOR PUBLICATION
18 March 2021

PUBLISHED
15 April 2021

PAPER

Appearance of objectivity for NV centers interacting with dynamically polarized nuclear environment

Damian Kwiatkowski[1,2,3,*], **Łukasz Cywiński**[1] and **Jarosław K. Korbicz**[4]

[1] Institute of Physics, Polish Academy of Sciences, al. Lotników 32/46, PL 02-668 Warsaw, Poland
[2] QuTech, Delft University of Technology, 2628 CJ Delft, The Netherlands
[3] Kavli Institute of Nanoscience, Delft University of Technology, 2628 CJ Delft, The Netherlands
[4] Centre for Theoretical Physics, Polish Academy of Sciences, al. Lotników 32/46, PL 02-668 Warsaw, Poland
[*] Author to whom any correspondence should be addressed.

E-mail: d.p.kwiatkowski@tudelft.nl

Keywords: nitrogen-vacancy center, open quantum systems, quantum control, quantum Darwinism

Abstract

Quantum-to-classical transition still eludes a full understanding. Out of its multiple aspects, one has recently gained an increased attention—the appearance of objective world out of the quantum. One particular idea is that objectivity appears thanks to specific quantum state structures formation during the evolution, known as spectrum broadcast structures (SBS). Despite that quite some research was already performed on this strong and fundamental form of objectivity, the practical realization of SBS in a concrete physical medium has not been explicitly analyzed so far. In this work, we study the possibility to simulate objectivization process via SBS formation using widely studied nitrogen-vacancy centers in diamonds. Assuming achievable limits of dynamical polarization technique, we show that for high, but experimentally viable polarizations ($p > 0.5$) of nuclear spins and for magnetic fields lower than ≈ 20 G the state of the NV center and its nearest polarized environment approaches an SBS state reasonably well.

1. Introduction

The central spin model—of a two-level system interacting with many other spins—is not only a paradigmatic model of decoherence [1, 2], but it has been highly relevant for description of dephasing of many kinds of semiconductor-based electron spin qubits interacting with nuclear spins [3–7]. Dynamics of nuclear-induced decoherence has been understood to a very large degree for many kinds of spin qubits interacting with nuclear environments consisting of between $\sim 10^2$ to $\sim 10^6$ nuclei [5, 7, 8]. For nitrogen-vacancy (NV) centers in diamond [9, 10] we are dealing with rather small environment of few hundreds of spins. The spin qubit based in this center has been extensively studied theoretically and experimentally in order to characterize its spin environment (both natural, consisting of spins of ^{13}C isotope [11, 13, 14], and artificially modified by putting organic molecules on top of the diamond [15, 16]) by analyzing the time-dependence of dephasing of an appropriately driven qubit [17]. Most importantly for us here, a large progress has been made in controlling the state of at least a part of this environment—up to a few tens of nuclear spins most strongly coupled to the central spin (the qubit)—and using the center to sense the state of at least some of these environmental spins. Having a well-tested theoretical model of open system dynamics for NV centers interacting with their nuclear environment [8, 18], one can shift the focus from the process of qubit's loss of coherence, to the possibly accompanying processes of modification of environmental state due to interaction with the qubit.

In the process of decoherence, qubit can leave traces of its presence in the environment. If we treat the environment as a channel through which many observers can acquire information about the qubit, then we can try to find how objectively this information is proliferated. Objectivity, as an important part of the quantum-to-classical transition, has been recently receiving a growing research attention, see e.g. [19–21, 25–28] for recent developments. The problem of objectivity, i.e. how to explain a robust objective world of

everyday experience from quantum postulates, was first raised by Zurek and collaborators [29, 30], who realized that decoherence alone is not enough, as nothing *a priori* guarantees that during its course information about the decohering system will make it into its environment in many copies accessible to independent observations—a prerequisite of objectivity. There have been proposed several approaches to the problem, with quantum Darwinism [29, 30] being the first and the most popular one, followed by spectrum broadcast structures (SBS) [31, 32, 35–39] and strong quantum Darwinism [40]. All the approaches can be viewed as extensions of theory of decoherence, in which one is interested not only in the system's state but also in what information about it, leaks into the environment (assumed to be a compound quantum system itself). The first and the last approaches study the behavior of quantum mutual information between the system and the parts of the environment, while SBS concerns directly the structure of quantum states. The rigorous relationships among them have been shown in [40]: SBS and strong Darwinism both imply the original quantum Darwinism but not vice versa since the original quantum Darwinism is in a sense too weak a condition for classicality as it can still allow for information not accessible locally (via quantum discord) (see also [41, 42]). The difference between SBS and the strong quantum Darwinism is in turn rather small, with the latter allowing for a bit more general, correlated structure of the environment (a fact already noted in [32] and thus both can be regarded as largely equivalent. A more detailed account of different approaches can be found in [42]. Since strong quantum Darwinism requires calculations of quantum discord, which are in general difficult, we will use in this work SBS formation as an indicator of objectivity.

Let us briefly recall [31, 32] that SBS are the following multipartite state structures:

$$\hat{\rho}_{Q:E_{\mathrm{obs}}} = \sum_m \pi_m \left|m^Q\right\rangle \left\langle m^Q\right| \otimes \hat{\rho}_m^{E_1} \otimes \ldots \otimes \hat{\rho}_m^{E_N}, \tag{1}$$

where E_{obs} is the observed part of the environment, π_m are probabilities, $\left|m^Q\right\rangle$ are so called pointer states to which the central system decoheres [1, 43] and the system state conditional density matrices of environmental parts must have mutually orthogonal supports and as a result be perfectly distinguishable:

$$\hat{\rho}_m^{E_k} \perp \hat{\rho}_{m'}^{E_k}. \tag{2}$$

It is straightforward to see that due to (2) each fragment of the environment perfectly encodes the same pointer state index m and it is locally measurable without any disturbance (on average) to the whole state (6). But this is nothing else than an operational form of objectivity [30] or to be more precise intersubjectivity [36]. Surprisingly, the converse is also true [32]: SBS (possibly generalized to correlated environments [40]) is the only state structure compatible with the quoted notion of objectivity. Interestingly, recent experiments [27, 28] that tested quantum Darwinism did so through SBS states [42].

We will discuss the formation of SBS structures in the experimentally widely investigated system of NV centers in diamond. It is worth mentioning at this point that recently a state of the art experiment has been performed [26], reporting an emergence of a (somewhat reduced) form of quantum Darwinism in NV system. While undoubtedly pioneering and of a great importance, in the light of the above discussion it represents rather the first step in using NV systems as 'simulators of objectivity'. In particular, SBS represents the strongest form of objectivity and it is an interesting question if NV centers can simulate it.

The electronic energy levels of these centers lie in the bandgap of diamond, and the ground state manifold of the NV center corresponds to spin $S = 1$ (e.g. [9]) system. The selection rules for coupling of photons to relevant transitions allow for optical initialization of spin-polarized state within the ground state manifold. By choice of microwave resonant drive between two out of three possible spin levels, one can experimentally define a qubit. Additionally, very weak spin–orbit coupling causes that the NV center decoherence is caused mostly by coupling to the environment formed out of ^{13}C nuclear spins randomly uniformly distributed through the lattice structure [18]. Natural concentration of those nuclei is around 1.1%, so the environment consists of rather sparsely distributed spins, the spatial arrangement of which does not reflect the periodicity of underlying crystal lattice. These spins are coupled to the NV center qubit, and also among themselves, via anisotropic dipolar interactions, whose power-law $(1/r^3)$ decay with distance, makes nearby spins much more strongly coupled than the remote ones, but does not allow for treating the interaction as having a finite range. This, together with the sparsity of the environment, means that the coupling constants in the Hamiltonian for each NV-environment system are specific to the given spatial arrangement of nuclei ('spatial realization of environment'). The experiments are most often done at finite magnetic fields, so the environmental spins undergo Larmor precession. The resulting dynamics due to this precession, qubit-nuclear coupling, and inter-nuclear interactions, strongly depends on the value of magnetic field. In the case on which we are focusing here—that of freely evolving qubit not subjected to any kind of dynamical decoupling that prolongs its coherence time [8]—complete dephasing of the qubit

occurs on timescale on which inter-nuclear interactions play no role [18]. However, the SBS emerge only after a time of decoherence caused by a part of the environment [31], which is longer than the time of decoherence due to the whole environment. Consequently, we will pay here careful attention to relevant timescales, in order to maintain the validity of approximation of treating the nuclear spins as mutually non-interacting.

For typically used values of magnetic field and temperature, the nuclear density matrix is very close to a completely mixed one. SBS cannot form with an initially completely mixed state of environment for a simple reason that such environment is completely ignorant to any information about the system and there is no chance for the condition (2) to be fulfilled (see e.g. [31, 44]). However, there has been a recent progress in generation of so-called dynamical nuclear polarization (DNP) of the nuclear spins most strongly coupled (i.e. the closest) to the NV center [45–54]. Consequently, we focus here on the case in which such a DNP is present, and we analyze the emergence of SBS as a function of polarization of the nuclei, and the size of the polarized fraction of the environment. A novel aspect of our SBS analysis is the inclusion of a non-trivial dynamics for the spin environment. This is an important generalization of the spin–spin models studied so far in the context of SBS fomation [36, 55]. In these studies, the environment self-Hamiltonian was completely neglected, leading to a very simplified and a rather academic model. Here we present a more realistic one (cf [33, 34]).

The work is organized in the following way. In section 2, we shall present the Hamiltonian for an NV center interacting with an environment of ^{13}C nuclei. In section 3 we first study a general model of SBS formation in spin systems with a non-trivial environment dynamics. We also discuss the model of the nuclear environment. We then apply the model to the situation when the nuclear environment interacts only with the central qubit, i.e. there are no direct interactions between the bath spins. In section 4 we perform numerical analysis of the model described in the prior sections, showing the regime of SBS formation under realistic conditions for NV centers in diamond with natural concentration of ^{13}C nuclei. Concluding remarks are presented in section 5.

2. The model

The system of the NV center and its nuclear environment is described by a pure dephasing Hamiltonian:

$$\hat{H} = \hat{H}_{\mathrm{Q}} + \hat{H}_{\mathrm{E}} + \hat{S}_z \hat{V} \tag{3}$$

where $\hat{H}_{\mathrm{Q}}$ is the Hamiltonian of the qubit, $\hat{H}_{\mathrm{E}}$ of the environment, $\hat{S}_z$ is the z component of center's spin (with z axis being determined by the vector connecting the nitrogen and the vacancy), and V is the environmental operator that couples to the qubit. A special feature of the NV center is that its low-energy subspace relevant for qubit physics is that of spin 1, so that $\hat{S}_z$ has eigenvalues $m = -1, 0, 1$. The qubit's Hamiltonian is

$$\hat{H}_{\mathrm{Q}} = \Delta_0 \hat{S}_z^2 + \bar{\Omega} \hat{S}_z, \tag{4}$$

where $\Delta_0 = 2.87$ GHz is the zero-field splitting, between the $m = 0$ and $m = \pm 1$ states, and $\bar{\Omega} = \gamma_{\mathrm{e}} B$ GHz is the Zeeman splitting between $m_{\mathrm{s}} = \pm 1$ levels due to external magnetic field B. Gyromagnetic ratio of the electron is equal to $\gamma_{\mathrm{e}} = 28.07$ GHz T^{-1}. Note that the B field is assumed to be parallel to the NV center quantization axis. There is a freedom of choosing any 2 out of 3 energy levels to define the qubit. Here we focus on the most popular (due to experimental ease of manipulation) choice of qubit based on $m = 0$ and $m = -1$ levels.

The environmental Hamiltonian consists of the Zeeman splittings term and the inter-nuclear interactions:

$$\hat{H}_{\mathrm{E}} = \sum_i \omega_i \hat{I}_z^i + \hat{H}_{\mathrm{int}}, \tag{5}$$

where $\omega_i = \gamma_{^{13}\mathrm{C}} B$ MHz is the Zeeman splitting with gyromagnetic ratio of ^{13}C nuclei, $\gamma_{^{13}\mathrm{C}} = 10.71$ MHz T^{-1}, and $\hat{I}_z^{(i)}$ is the z-axis spin operator of the ith nuclear spin. There are two mechanisms of electronic spin-nuclear spin coupling: Fermi contact interaction, which is proportional to the overlap of the electronic wavefunction at the position of a nucleus $A_{\mathrm{Fermi}} \propto |\psi_{\mathrm{e}}(\mathbf{r}_i)|^2$, and dipolar interaction. The former is negligible for nuclei farther away than 0.5 nm from the center [56] as the wavefunction is highly localized for deep defects. Within this radius, for $\approx 50\%$ possible realizations of the environment there will be no spinful nuclei. Keeping in mind the post-selection of spatial realizations of the environment that needs to be done, we will focus from now on only on dipolar qubit-nuclear spin couplings.

For magnetic fields of interest here, the order of magnitude of qubit energy splitting is determined by the zero-field splitting Δ_0, which is much larger than the nuclear energy scales (Zeeman splittings, dipolar

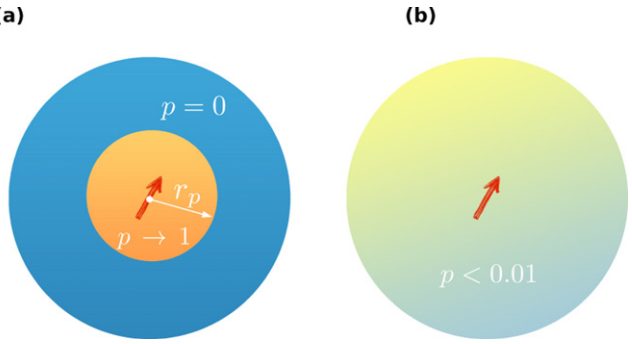

Figure 1. Experimental strategies for nuclear polarization in NV centers. Panel (a) depicts a situation when strongly coupled nuclei, located up to a radius $r_{\rm p}$ from the NV center, are polarized using DNP. Panel (b) shows the case for achieving a polarization in high magnetic fields and cryogenic temperatures to increase the ratio between Zeeman splitting and temperature, which corresponds to thermal polarization $p_i = \tanh(\omega_i/2k_{\rm B}T)$. In this work we study case (a), unless otherwise stated.

interactions). Consequently, the qubit and its environment cannot exchange energy, i.e. we are dealing with pure dephasing, and we can neglect terms $\sim \hat{S}_x, \hat{S}_y$ in the qubit-nuclear coupling, which is therefore given by

$$\hat{S}_z \otimes \hat{V} = \sum_k \sum_{j=x,y,z} \hat{S}_z \otimes A_k^j \hat{I}_j^k \,, \tag{6}$$

where $j = x, y, z$ enumerates directions of spin operators, k-nuclear spins interacting with the qubit and A_k^j are given by:

$$A_k^j = \frac{\mu_0 \gamma_{\rm e} \gamma_{^{13}{\rm C}}}{4\pi} \frac{\hat{\mathbf{z}} \cdot \hat{\mathbf{j}}}{|\mathbf{r}_k|^3} - \frac{3(\hat{\mathbf{z}} \cdot \mathbf{r}_k)(\hat{\mathbf{j}} \cdot \mathbf{r}_k)}{|\mathbf{r}_k|^5}, \tag{7}$$

where μ_0 is the magnetic permeability of vacuum, $\mathbf{r}_k$ is a displacement vector between nitrogen and nucleus k and the gyromagnetic ratios $\gamma_{\rm e}$ and $\gamma_{^{13}{\rm C}}$ are defined above.

For qubit based on $m = 0$ and 1 levels that we consider here, the qubit-environment coupling is then given by $|0\rangle\langle 0| \otimes \hat{V}_0 + |1\rangle\langle 1| \otimes \hat{V}_1$ in which

$$\hat{V}_m = m \sum_k \sum_{j=x,y,z} A_k^j \hat{I}_j^k, \tag{8}$$

so that $\hat{V}_0 = 0$. Consequently, the evolution operator of the whole system can be written as:

$$\hat{U}(t) = |0\rangle\langle 0| \otimes \hat{\mathcal{U}}_0(t) + |1\rangle\langle 1| \otimes \hat{\mathcal{U}}_1(t) \,, \tag{9}$$

where the conditional evolution operators are given by

$$\hat{\mathcal{U}}_m(t) = \exp[-{\rm i}t(\hat{H}_{\rm E} + \hat{V}_m)]. \tag{10}$$

We are working in the qubit rotating frame, so that the energy splitting of the qubit $\bar{\Omega} + \Delta_0$ is removed.

Having discussed the dynamics, let us now discuss the initial conditions. If the spin environment is non-polarized, the interaction (9) will not lead to any information recording in the environment, only to dephasing [22, 23, 57]. Therefore we will consider here partially polarized environments. Specifically, we focus on environments in which nuclear spins within some distance from the qubit are polarized, as such an environmental state can be prepared by repetition of appropriate manipulation protocols [45–54] on the qubit and the nuclei, and the efficiency of polarization scales with the magnitude of qubit-nuclear coupling. Such an initial state of the environment is illustrated in figure 1. Another strategy for nuclear polarization is to put the diamond crystal in cryogenic temperatures and apply high magnetic field, resulting in uniform polarization after the nuclear spins reach thermal equilibrium with the lattice, see figure 1(b). However, equilibrium polarization p for temperature of a few tens of milikelvins and at $B \sim 1$ T is $p \sim 10^{-2}$. Below we will see that such a polarization is not enough to support formation of the SBS.

3. Dynamics of the SBS formation

3.1. General considerations

As explained in the Introduction, our method is based on direct studies of the quantum state as the most fundamental carrier of information. In particular, we are interested if there are regimes such that a joint

state of the central qubit and some of its nuclear environment approaches the SBS structure (6) and (2), signalizing that the state of the qubit acquired a certain operational objective character during the evolution as explained in detail in [31, 32]. As in the previous SBS studies, e.g. in [31, 35, 36, 55], our method is the following. First, since we are interested not only in the state of the qubit alone but in how it is correlated with some of its environment, we cannot trace all of the environment as it is normally done. Instead, we divide the environment E into two parts: the one we are interested in (say observed), denoted symbolically fE and containing fN spins, $0 \leqslant f \leqslant 1$, and the one that pass unobserved and can be traced out, denoted $(1-f)E$ and containing the rest of the $(1-f)N$ nuclei. In terms of experimental capabilities, one may think of DNP as a form of environment separation. As described above, high degree of polarization can be reached for only a few nuclear spins closest to the NV center. Control and observation of polarized fragment of the environment can be realized by measurement $\langle\hat{\sigma}_y\rangle$ of the qubit as a function of total evolution time, which is zero when the environment is completely mixed during evolution of a qubit initialized in eigenstate of $\hat{\sigma}_x$.

The main object of our study is what we call a partially reduced state:

$$\hat{\rho}_{Q:fE}(t) = \mathrm{Tr}_{(1-f)E}\,\hat{\rho}_{Q:E}(t), \tag{11}$$

obtained by tracing out only the unobserved part of the environment, $(1-f)E$, from the global qubit-environment state $\hat{\rho}_{Q:E}(t)$ evolving under (9). The check for SBS structure then proceeds in two steps [36]: (i) first check if dephasing takes place and the partially reduced state approaches the form equation (6); (ii) check if the conditional environment states satisfy (2). The first condition, dephasing, is fairly standard and we will use well-known results, scaled down however to a part of the environment rather than the whole. When it comes to the second condition, out of the several available measures of state distinguishability (2) [24], we use the state fidelity:

$$\mathcal{F}(\hat{\rho},\hat{\sigma}) = \mathrm{Tr}(\sqrt{\hat{\rho}}\hat{\sigma}\sqrt{\hat{\rho}}) \tag{12}$$

for the ease of work. In any case, we are interested only in $\mathcal{F}=0$, which is equivalent to (2). It can happen that a state of a single environment nucleus is changed too little during the evolution (9) to approach (2), but when we consider groups of nuclei, their joint states can come close to satisfying (2). This can be viewed as a kind of 'information concentration'. Anticipating such situation, we introduce following [31] a further coarse-graining of the observed environment fE into M groups, called macrofractions, each of a size $\mu N = (f/M)N$ (equal sizes are for our convenience only). The approach to SBS is then mathematically equivalent to simultaneous vanishing of the decoherence factor due to $(1-f)E$ and all the pairwise fidelities calculated between the states of the macrofractions [36]. We note that for pure states the fidelity (12) becomes just the overlap between the two considered states $F(\psi,\phi) = |\langle\psi|\phi\rangle|^2$.

The concrete setup studied here will be the DNP setup of figure 1(a) with the following identifications:

- The central system is the NV qubit, defined by the $|m^{\mathrm{Q}}=0\rangle$ and $|m^{\mathrm{Q}}=1\rangle$ states, which constitute the pointer basis. We are seeking if during the interaction with the environment, the decohered state of the qubit becomes objective via a creation of the SBS state (6).
- The observed part of the environment, fE, will be the DNP spins within the radius r_{p} from the NV center.
- The observed part will be further divided into several, equal size, macrofractions (see figure 2). They represent parts of the environment accessible for independent observers.
- The weakly polarized part of the environment past the radius r_{p} carries vanishingly small amount of information about the qubit and thus this will be the unobserved part, $(1-f)E$, subsequently traced over.

We assume that the initial state of the qubit and all the nuclei is initially completely uncorrelated:

$$\hat{\rho}_{Q:E}(0) = \hat{\rho}_Q(0)\otimes\hat{\rho}_E(0) = \hat{\rho}_Q(0)\bigotimes_k\hat{\rho}_E^k(0)\,, \tag{13}$$

where k enumerates nuclei in the bath, and the state of a single nucleus is given by

$$\hat{\rho}_E^k(0) = \frac{1}{2}(\mathbb{1} + p_k\hat{\sigma}_z^{(k)})\,, \tag{14}$$

in which p_k is the initial polarization degree. When $p_k = \pm 1$, the state is pure, and when $p_k = 0$, the state is fully mixed. In other words, only spins affected by DNP, thus, forming the observed environment, will correspond to $p_k \neq 0$ and for the unobserved part, we assume $p_k = 0$, corresponding to room temperature—typical conditions for experiments with NV centers.

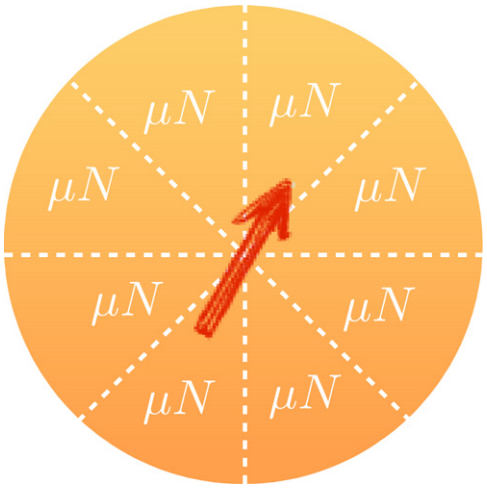

Figure 2. Schematic representation of the coarse-graining of the observed part of the environment, fE, into macrofractions containing μN spins each. This helps achieving 'information concentration', defined here by the perfect distinguishability of the states (2), and thus helps approaching SBS states. This is more general situation than just considering each environmental spin individually.

Anticipating the irrelevance of inter-nuclear interactions, the total Hamiltonian reads:

$$\hat{H} = (\Delta_0 + \bar{\Omega})\,|1\rangle\langle 1| + \sum_k \omega_k \hat{I}_z^k + |1\rangle\langle 1| \otimes \sum_k \sum_{j=x,y,z} A_k^j \hat{I}_j^k. \tag{15}$$

This Hamiltonian allows for a correct description of decoherence of a freely evolving NV center spin qubit [18], which has also been used for interpretation of experimental signal from such an NV center [58]. From the point of view of objectivity and SBS studies, the above Hamiltonian is an important generalization of the previously studied spin–spin models [36, 55].

When the central qubit is initialized in a pure superposition of pointer states, i.e. in

$$\hat{\rho}_Q(0) = |\phi\rangle_Q\langle\phi|, \qquad |\phi\rangle_Q = c_0|0\rangle + c_1|1\rangle, \tag{16}$$

the evolution of total system, governed by (9), is given by:

$$\hat{\rho}_{Q:E}(t) = \sum_{m,m'=0,1} c_m c_{m'}^* |m^Q\rangle\langle m'^Q| \bigotimes_{k=1}^{N} \hat{\mathcal{U}}_m^k \hat{\rho}_E^k(0) \hat{\mathcal{U}}_{m'}^{k\dagger}. \tag{17}$$

3.2. Analytical results-decoherence factor

Once we trace out the unobserved part of the environment $(1-f)E$, the partially reduced density matrix becomes:

$$\hat{\rho}_{Q:fE}(t) = \sum_{m=0,1} |c_m|^2 |m\rangle_Q\langle m| \bigotimes_{k=1}^{fN} \hat{\mathcal{U}}_m^k \hat{\rho}_E^k(0) \hat{\mathcal{U}}_m^{k\dagger} + \left(c_m c_{m'}^* \gamma_{mm'}(t) |m\rangle_Q\langle m'| \otimes \bigotimes_{k=1}^{fN} \hat{\mathcal{U}}_m^k \hat{\rho}_E^k(0) \hat{\mathcal{U}}_{m'}^{k\dagger} + \text{c.c.} \right). \tag{18}$$

where $\gamma_{mm'}(t)$ is the decoherence factor coming from the unobserved fraction of the environment $(1-f)E$. For the chosen realization of a qubit between $m = 0$ and $m = 1$ states, this term can be expressed as:

$$\gamma(t) = \prod_{k=1}^{(1-f)N} \gamma_k(t) = \prod_{k=1}^{(1-f)N} \text{Tr}\left(\hat{\mathcal{U}}_0^k \hat{\rho}_k^E(0) \hat{\mathcal{U}}_1^{k\dagger}\right), \tag{19}$$

where the single nucleus decoherence factor $\gamma_k(t)$ reads by (8)–(10):

$$\gamma_k(t) = \cos\frac{\omega_k t}{2}\cos\frac{\Omega_k t}{2} + \frac{A_k^z+\omega_k}{\Omega_k}\sin\frac{\omega_k t}{2}\sin\frac{\Omega_k t}{2} + \mathrm{i}p_k\left(\cos\frac{\Omega_k t}{2}\sin\frac{\omega_k t}{2} - \frac{A_k^z+\omega_k}{\Omega_k}\cos\frac{\omega_k t}{2}\sin\frac{\Omega_k t}{2}\right) \tag{20}$$

in which $\Omega_k = \sqrt{\left(A_k^{\perp}\right)^2 + (\omega_k + A_k^z)^2}$ and $A_k^{\perp} = \sqrt{\left(A_k^x\right)^2 + \left(A_k^y\right)^2}$. The modulus is given by:

$$|\gamma_k(t)|^2 = \left[1-(1-p_k^2)\sin^2\frac{\omega_k t}{2}\right]\cos^2\frac{\Omega_k t}{2} + \left(\frac{A_k^z+\omega_k}{\Omega_k}\right)^2\left[1-(1-p_k^2)\cos^2\frac{\omega_k t}{2}\right]\sin^2\frac{\Omega_k t}{2} + \frac{A_k^z+\omega_k}{2\Omega_k}(1-p_k^2)\sin(\omega_k t)\sin(\Omega_k t). \tag{21}$$

A general expression for decoherence factor when qubit is defined between m and m' states can be found in appendix A.

We now have to estimate the product (19) with the factors given by (20). Analytical studies are possible only under some simplifications. The most universal one is the short-time limit $\Omega_k t \ll 1$, which also implies $\omega_k t \ll 1$, so it can hold only below a certain magnetic field for given timescale of interest. The total decoherence factor then reads:

$$\gamma^{\mathrm{weak}}(t) \approx \exp\left[-\left(t/T_2^*\right)^2 - \mathrm{i}\phi(t)\right] \tag{22}$$

where the dephasing time T_2^* is defined by

$$(T_2^*)^2 = \frac{8}{(1-f)N\langle (A^z)^2 + (A^{\perp})^2\rangle}, \tag{23}$$

and the phase shift is given by $\phi(t) = (1-f)N\langle pA^z\rangle t/2$. The averages are defined by:

$$\langle g(A)\rangle = \frac{1}{(1-f)N}\sum_k^{(1-f)N} g(A_k). \tag{24}$$

As expected, at short times the decoherence factor shows a Gaussian decay but this does not mean that it decays also for larger times. In fact in general it does not for small traced fractions. However analytical study of mid/long-time behavior is very difficult due to the complicated nature of the functions (19) and (20) and therefore for the purpose of this work a further analysis of $\gamma(t)$ will be carried out numerically.

3.3. Analytical results-conditional states fidelity

After the decoherence due to the unobserved part of the environment has taken place, the resulting partially traced state (18) comes close to the SBS form (6). We have to however still check the orthogonality (2) for the conditional states $\hat{\rho}_m^{E_k} \equiv \hat{\rho}_m^k$, where $\hat{\rho}_m^k(t) = \hat{\mathcal{U}}_m(t)\hat{\rho}_E^k(0)\hat{\mathcal{U}}_m^{\dagger}(t)$, cf (18). We will use the state fidelity function (12). We calculate it, using the fact that all the matrices are 2×2:

$$\mathcal{F}_{mm'} = \mathcal{F}\left(\hat{\rho}_m^k(t), \hat{\rho}_{m'}^k(t)\right) = \mathrm{Tr}[\hat{\rho}_m^k(t)\hat{\rho}_{m'}^k(t)] + 2\sqrt{\det[\hat{\rho}_m^k(t)]\det[\hat{\rho}_{m'}^k(t)]}. \tag{25}$$

For the qubit based on $m\in\{0,+1\}$ levels, considered here, the resulting fidelity for conditional states of the nucleus becomes:

$$\mathcal{F}\left(\hat{\rho}_0^k(t), \hat{\rho}_1^k(t)\right) = 1 - \frac{\left(A_k^{\perp}\right)^2}{\Omega_k^2}p_k^2\sin^2\left(\frac{\Omega_k t}{2}\right), \tag{26}$$

While single-spin contribution to decoherence, equation (20), is finite even when $A_k^{\perp}=0$ (only nonzero A_k^z is needed), for the fidelity between the two conditional states of a single environmental spin to be less than unity, $A_k^{\perp}\neq 0$ is necessary. This is a consequence of a simple observation that the environment has to undergo an evolution non-trivially conditioned on the state of the qubit for this fidelity to deviate from unity. We recall that fidelity equals to one iff the states are identical, which is a trivial situation. For the similar reason, the non-polarized limit of $p_k\to 0$ is not interesting either.

In the studied model of qubit-environment coupling leading to qubit's pure dephasing, and initially pure state of the qubit, the necessary condition for the conditional states to be (approximately) orthogonal at long enough times is appearance of nonzero qubit-environment entanglement at earlier times, in the

initial stages of the evolution [12]. The condition for the latter is $\hat{\rho}_0^k(t) \neq \hat{\rho}_1^k(t)$, as shown in [57, 59]. This motivates why as the observed part of the spin environment we consider only the polarized part. These are the nuclear spins inside a ball of radius r_p, schematically shown in figure 1, according to experimental state of the art concerning DNP.

As we explained at the beginning of this section, to increase the chances of satisfying distinguishability condition (2), we perform a coarse-graining of the observed environment fE, dividing it into M macrofractions of size μN each. Symbolically $fE = \mu E \cup \cdots \cup \mu E$. The state of each macrofraction for neglected mutual interactions is just a product $\hat{\rho}_m^{\mu E}(t) \equiv \bigotimes_{k\in\mu N} \hat{\rho}_m^k(t)$ so that using the factorization property of the fidelity we obtain:

$$\mathcal{F}_{mm'}^{\mu E}(t) \equiv \mathcal{F}\left(\hat{\rho}_m^{\mu E}(t), \hat{\rho}_{m'}^{\mu E}(t)\right) = \prod_{k\in\mu E} \mathcal{F}\left(\hat{\rho}_m^k(t), \hat{\rho}_{m'}^k(t)\right). \tag{27}$$

Thus, the fidelity between two qubit-state conditional density matrices of macrofractions is a product of contributions from equation (26):

$$\mathcal{F}^{\mu E}(t) = \prod_{k\in\mu E}\left[1 - p_k^2 \frac{\left(A_k^\perp\right)^2}{\Omega_k^2} \sin^2\left(\frac{\Omega_k t}{2}\right)\right]. \tag{28}$$

A general expression for a qubit defined between m and m' is much more complicated and can be found in appendix B.

We are now interested when $\mathcal{F}^{\mu E}(t) \to 0$, meaning the condition (2) is satisfied for macrofraction states. The easiest regime for analytical study corresponds to a situation, when:

$$\frac{\left(A_k^\perp\right)^2}{\Omega_k^2} p_k^2 \sin^2\left(\frac{\Omega_k t}{2}\right) \ll 1 \tag{29}$$

for every k. This happens when e.g. (i) all the members of the macrofraction are weakly coupled to the central spin:

$$\frac{\left(A_k^\perp\right)^2}{\Omega_k^2} \ll 1 \Leftrightarrow \frac{A_k^z + \omega_k}{A_k^\perp} \gg 1, \tag{30}$$

or when (ii) polarization of the observed environment is low, meaning:

$$p_k^2 \ll \frac{\Omega_k^2}{\left(A_k^\perp\right)^2} = 1 + \frac{(A_k^z + \omega_k)^2}{\left(A_k^\perp\right)^2}, \tag{31}$$

or when (iii) we consider very short times $\Omega_k t \ll 1$. Then, equation (28) can be rewritten as an exponential of a sum of contributions from all the nuclei in the macrofraction:

$$\mathcal{F}^{\mu E}(t) \approx \exp\left[-\sum_{k=1}^{\mu N} \frac{\left(A_k^\perp\right)^2}{\Omega_k^2} p_k^2 \sin^2\left(\frac{\Omega_k t}{2}\right)\right]. \tag{32}$$

For short times $\Omega_k t \ll 1$, we can derive an effective timescale of the initial decay of the fidelity:

$$\mathcal{F}^{\mu E}(t) \approx \exp\left[-\frac{1}{4}\sum_{k=1}^{\mu N} p_k^2 \left(A_k^\perp\right)^2 t^2\right] = \mathrm{e}^{-\left(\frac{t}{\tau_\mu}\right)^2}, \tag{33}$$

where

$$\tau_\mu^{-2} = \frac{1}{4}\mu N \langle p^2 A_\perp^2 \rangle_{\mu N}, \tag{34}$$

with $\langle\cdot\rangle_{\mu N}$ denoting the averaging over the macrofraction, similar to (24). In general, to prove the orthogonalization (2), this short time analysis is of course not enough. As for the behavior of fidelity at long times, we can state the following. Let us assume that:

$$\Omega_k \approx \omega + \frac{\left(A_k^\perp\right)^2}{2\omega} \tag{35}$$

(with Zeeman splittings ω_k assumed to be the same ω for all the nuclei, implying spatially uniform magnetic field), which holds for $\omega \gg A_k^\perp, A_k^z$. This automatically implies (29) via (30) so that we can use (32). With σ being the standard deviation of distribution of $A_k^\perp$ in the given macrofraction, for $\sigma^2 t/2\omega \gg 1$

the values of $\sin^2\Omega_k t/2$ in equation (32) are randomly distributed in $[0, 1]$. With many spins in the macrofraction, we can replace then $\sin^2\Omega_k t/2$ terms by their average value of $1/2$, and the fidelity is

$$\mathcal{F}^{\mu E}_{mm'}\left(t \gg \frac{2\omega}{\sigma^2}\right) \approx \exp\left[-\frac{1}{2\omega^2}\sum_{k=1}^{\mu N}\left(A_k^{\perp}\right)^2 p_k^2\right]. \tag{36}$$

If in the macrofraction of interest

$$\mu N \frac{\langle p^2 A_{\perp}^2\rangle_{\mu N}}{\omega^2} \gg 1, \tag{37}$$

which should be treated as a condition for minimal polarization or the number of spins in the macrofraction, then the fidelity decays towards a very small value on timescale that is $\sim \omega/\sigma^2$.

For a qubit with a macrofraction μN to form a spectrum broadcast structure, we not only need to meet a condition for mutual orthogonalization for conditional states of the macrofraction, but also decoherence due to the remaining part of the bath. For short times the ratio of the decoherence and orthogonalization time becomes:

$$\left(\frac{T_2^*}{\tau_\mu}\right)^2 = \frac{\mu}{1-f}\cdot\frac{2\langle p^2 (A^{\perp})^2\rangle_{\mu N}}{\langle (A^z)^2 + (A^{\perp})^2\rangle_{(1-f)N}}. \tag{38}$$

Experimental endeavor to measure and control clusters of polarized nuclear spins with NV centers is mostly limited by the decoherence of the NV center. Therefore, if decoherence happened on a longer timescale than orthogonalization, it should be possible to predict formation of SBS, e.g. by state tomography.

4. Numerical results

Analytical studies of the decoherence and the fidelity factors, derived in the previous section, are quite limited due to the fact that compact approximate expressions can only be obtained for weakly coupled ($\omega \gg A_k^z, A_k^{\perp}$) or weakly polarized nuclei—and below we will show that having large polarization and strong coupling is needed for appearance of genuine SBS. We will now present results of numerical investigations. We recall that in order to show the creation of SBS states, both functions (19) and (28) must vanish.

Experiments and theory of decoherence of NV centers show that the time-dependence of their dephasing is very prone to the effects connected with presence of a few, maybe few tens of strongly coupled nuclei, located 1–2 nm from the defect. A widespread collection of applications of such nuclei, either for sensing or creating a register for quantum networks have been discussed and tested experimentally [13, 60–62]. Presence of such 'fingerprints' of a spatial arrangement of environmental spins most strongly coupled to the qubit is also expected in the time-dependence of fidelity between the states of a macrofraction conditioned on two states of the qubit. Here we consider a given number fN of nuclear spins within a ball of radius r_{p} around NV center, which are in a polarized state. Outside of this region, the environment is initialized in a completely mixed state, which corresponds to room temperature conditions, typical for NV center experiments.

Numerical studies performed here are based on parameters of natural samples of diamonds implanted with NV centers. Diamond lattice symmetry corresponds to a diamond cubic crystal structure, with a cubic unit cell containing three tetrahedrons with carbon atoms as vertices. Each side of the unit cell corresponds to $a_{NN} = 0.357$ nm distance between the neighboring carbon atoms. For a given realization of the environment around an NV center positioned at one of these vertices, positions of spinful ^{13}C nuclei, described by lattice are drawn from a random uniform distribution of sets of three lattice indices, corresponding to spatial location of these species. Size of the environment, enumerated by number of spins in the environment-N-has to be estimated by the convergence of results for quantities of interest (decoherence factor due to unobserved fraction of the environment, fidelity between the conditional states for macrofractions) as function of size of part of environment taken into account, while considering these quantities on certain timescale (here determined by decoherence due to unobserved nuclei). Experimental and theoretical works show that NV centers should be sensitive to nuclei at distances of a few nanometers with natural concentration of ^{13}C isotope in the lattice [9, 13]. This corresponds to the total number of spins on the order of $N = 300$–500. We assume here $N = 400$. The dipolar couplings of nuclei to the NV center, i.e. $A_k^{\perp}$ and A_k^z, are then determined from equation (7) and are random quantities due to random positions $\mathbf{r}_k$. We assume equal Zeeman splittings $\omega_k = \omega$, corresponding to application of constant external magnetic field $B = 10$ G. Concerning polarization degrees, we assume an experimentally viable scenario of application of DNP as a preparatory stage, which results in the environment split into highly polarized and non-polarized parts as depicted in figure 1(a). We then associate the observed part of the environment fE, of the size fN, with the highly polarized fraction, assuming equal polarization for all spins in fE,

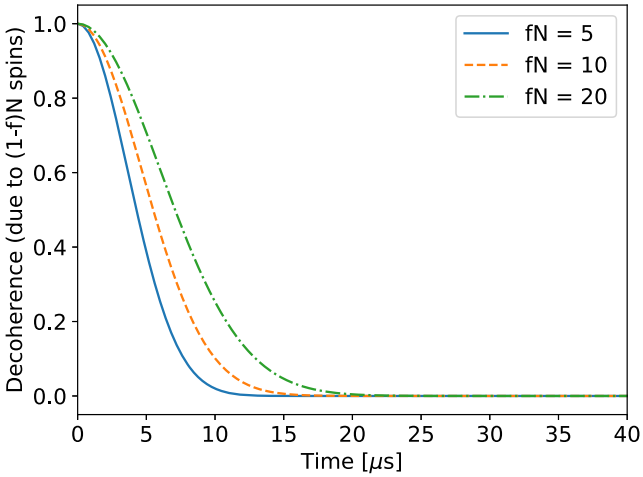

Figure 3. Modulus squared of the decoherence factor (19) as a function of time. The plot corresponds to a single spatial realization of nuclear environment, labelled as (II). Due to the fact that unobserved part of environment, used to generate the plot, does not contain by assumption strongly coupled nuclear spins, this figure can be treated as reference for decoherence timescales independently of realization. The total number of spins in the simulation is $N = 400$. Each curve is enumerated by the size of the observed macrofraction fE, rather than that of the unobserved $(1 - f)E$, hence the larger the fN the slower the decoherence as less nuclei out of the total $N = 400$ contribute to (19). The corresponding state fidelities are shown in column (II) of figure 4.

$\forall_{k\in fE}\, p_k = p \neq 0$. The unobserved part $(1 - f)E$, of the size $(1 - f)N$, is then the unpolarized fraction, assumed initially in a completely mixed state: $\forall_{k\in(1-f)E}\, p_k = 0$. Thus, the only randomness is in the coupling constants $A_k^{\perp}$ and A_k^{z}.

We will first look at the decoherence process as the necessary condition for the SBS formation. The choice of the unobserved environment by removing the strongly coupled nuclei from the decoherence function (19) means that decoherence as a function of time can be well-represented by one spatial realization of the environment (assuming no application of any resonant operations on the central qubit). Figure 3 shows the squared modulus of the decoherence factor (19) for a single sample realization, further denoted as (II), and different fully polarized (observed) fractions fN. All of these curves have been tested for relevance of intra-environment interactions, using the so called cluster-correlation expansion (CCE), using which one can account in a controllable way for influence of inter-nuclear interactions on qubit's decoherence [8, 13, 63, 64]. The calculations have shown that for magnetic field $B = 10$ G, it is sufficient to describe the decoherence dynamics due to the environmental remainder as non-interacting (CCE-1) on the timescales of $t < 300$ μs, which is in agreement with [13, 58]. Figure 3 shows a smooth Gaussian decay of coherences on the time scale of 10–20 μs, depending on how many of N nuclei are left for observation. In figure 5, where we analyze formation of SBS states for macrofractions of $fN = 5, 10, 20$ nuclear spins closest to the NV center, we also show decoherence computed, taking into account up to four-spin correlations generated by their mutual interactions (CCE-4) (dashed-green curves). Results confirm that treating the unobserved environment as non-interacting on these timescales is justified.

Let us now look at the state fidelity (28) for the polarized spins. The results are presented in figure 4. The first two columns show (28) as a function of total evolution time for two different spatial realizations of the nuclear environment in relatively low magnetic field of 10 G. As described earlier, nuclear spins are randomly uniformly distributed in the diamond lattice and their concentration is 1.1%. The rows (a)–(c) correspond to different polarizations, assumed the same for all the nuclei in the macrofraction. First of all, one can see that the polarization p plays a crucial role in the fidelity behavior and for low polarization, figure 4(a), there is no chance of approaching even remotely the state distinguishability (2) for any reasonable macrofraction size. This is because for low p the initial environment state is very close to the totally mixed stated (cf (14)) and hence is very little affected by the interaction. However, figures 4(b) and (c) show that for higher polarizations ($p > 0.5$), even a macrofraction of few dozens nuclei can achieve some level of distinguishability for times $t > 100$ μs given our assumed parameters. These plots also show the initial Gaussian decay of the fidelity as predicted by the short-time analysis of section 3.3. Past short times however, one can see an oscillatory behavior, especially prominent for small macrofraction sizes. This is due to the not enough randomization for small sizes μN of the strongly coupled nuclei.

In order to see more clearly the qualitative behavior of the fidelity, we present its average over a hundred realizations of the positions of the ^{13}C nuclei around the NV center in the last column of figure 4. Clearly,

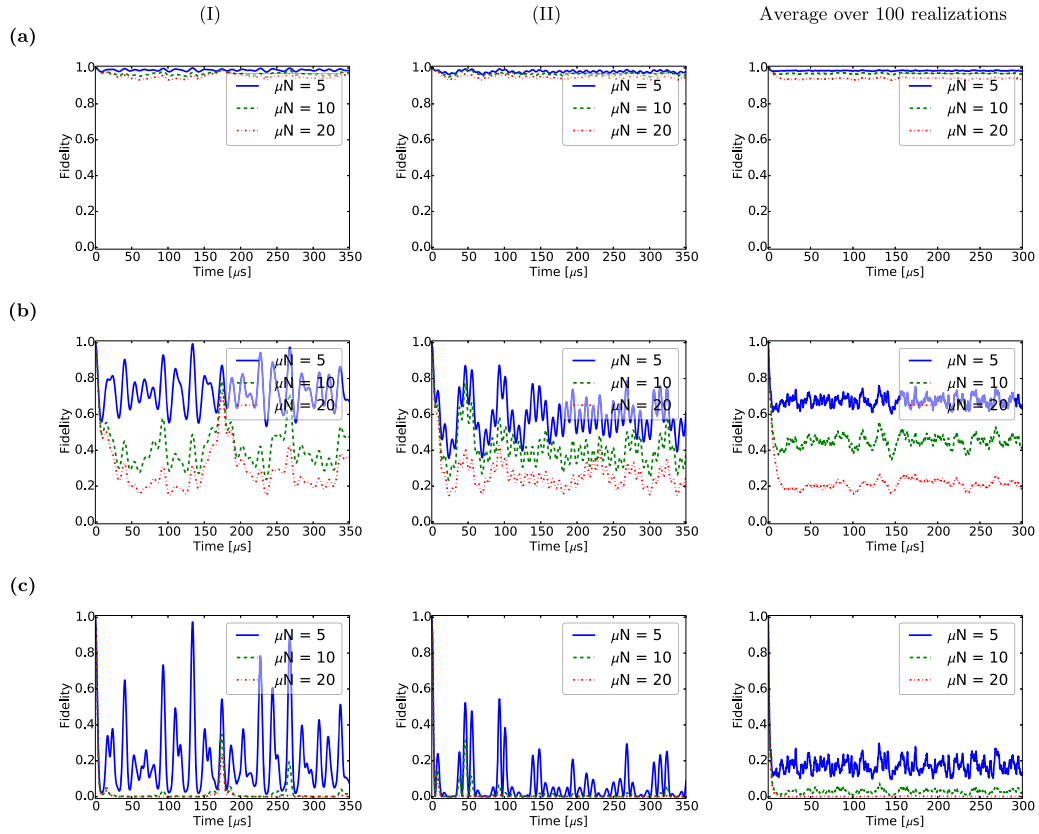

Figure 4. Fidelity as a function of evolution time for 2 spatial realizations, labelled (I) and (II), and an average over 100 realizations of the nuclear environment, corresponding to macrofractions containing $\mu N = 5$, 10, 20 nuclear spins. Panels (a)–(c) correspond to macrofraction polarizations $p = 0.1$, 0.5 and 1.0, respectively.

the orthogonalization of the conditional environmental states is both faster, and more complete, for larger polarizations and macrofraction sizes.

Comparing figures 3 and 4 (b) and (c) suggests there is a time region when both functions come reasonable close to zero, indicating that the partially reduced state is close to the SBS form. Indeed it is so as figure 5 shows. Working with the realization (II) from figure 4 for definiteness, we assumed the polarized (observed) fraction fE is divided into two identical macrofractions $fE = \mu E \cup \mu E$ of the size μN. We assume the polarization degree $p = 0.9$, which should be experimentally viable, close to achieving an initially pure state for the observed part of the environment. In the case of the division into $\mu N = 5$ spin-macrofractions (cf figure 5(a)), the fidelity strongly oscillates, indicating an insufficient number of spins in the macrofraction. However, for $\mu N = 10$, figure 5(b), although the fidelity shows some revivals for certain times, it generally tends to weakly oscillate around zero. For $\mu N = 20$, figure 5(c), the situation is even better with a definite decay of the fidelity past $t \approx 20$ μs. Therefore, we can claim that for macrofractions of at least 10 strongly coupled nuclear spins in the highly polarized ($p \geqslant 0.9$) part of the environment, an SBS state is approached within 100 μs. Since in the current state of the art experiments, a polarization of around 20 tightly coupled spins is achieved [62], the realistic SBS structure one can expect is a two-observer one.

For fractions of $\mu N = 5$, 10 (figures 5(a) and (b)), we also show numerical calculation of fidelity, including interactions between nuclear spins (yellow dashed lines). For the chosen external magnetic field and resulting timescales of SBS formation, interactions between nuclear spins do not play any significant role both in orthogonalization of conditional nuclear states, and (as discussed above) decoherence of the central spin due to the unobserved part of the environment.

All of the previous results have been calculated for a relatively low magnetic field of 10 G. When increasing the field, we should be able to suppress the dynamics of nuclear spins induced by transverse the hyperfine couplings—i.e. the dynamics that is caused by interaction with the qubit, and thus might be conditional on the state of the qubit. The dependence of the fidelity on the magnetic field is presented in figure 6 for a group of completely polarized 20 nuclear spins. For fields between 10-20 G, the fidelity only slightly deviates from zero, but for 50–100 G, it persistently oscillates, which means that only a few nuclear spins contribute to formation of mutually orthogonal conditional states and thus the formation of SBS is not observed. These few nuclear spins are the ones that are still *strongly coupled* to the qubit at elevated

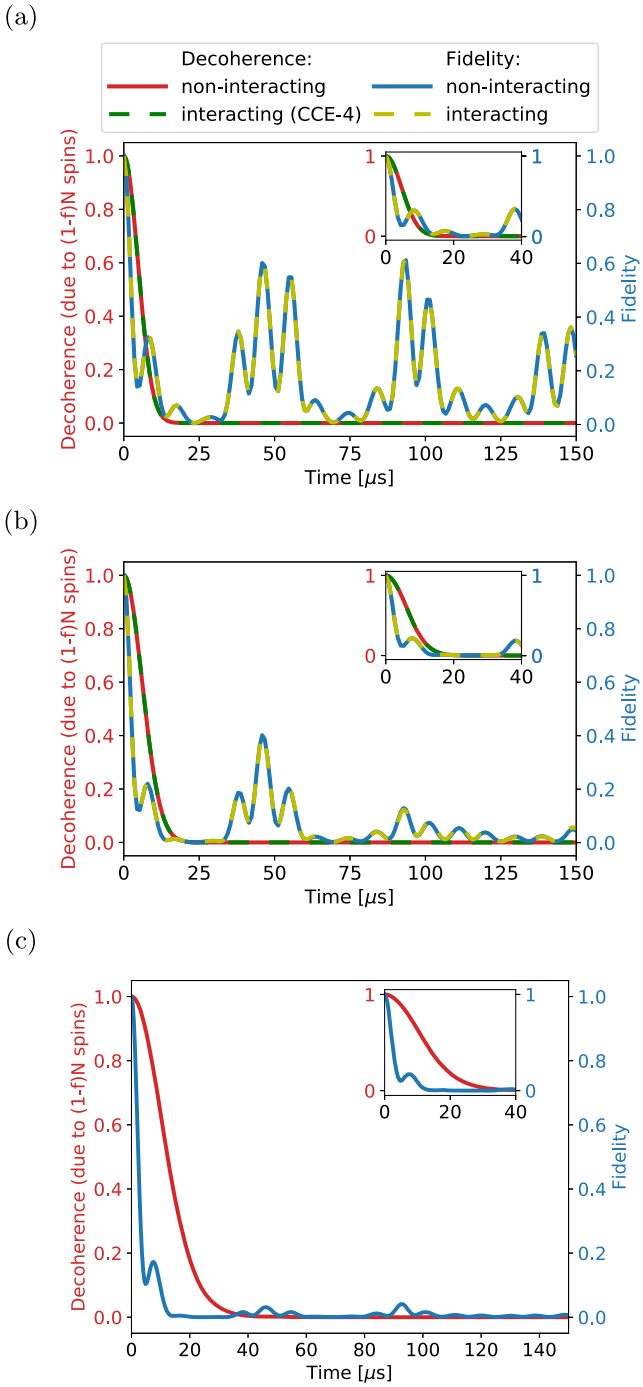

Figure 5. Example of SBS states formation. We assume realization (II) polarized up to $p = 0.9$. The strongly coupled fraction fN is divided into two identical fractions, $fN = 2 \times \mu N$, of a size: (a) $\mu N = 5$, (b) $\mu N = 10$ and (c) $\mu N = 20$. The blue curve corresponds to the fidelity and the red curve to decoherence due to the unobserved environment. Dashed green line shows decoherence calculation up to CCE-4 and dashed yellow line-fidelity, including internuclear couplings in the Hamiltonian. Total number of spins in the nuclear bath is $N = 400$. The insets show the short-time behavior that is close to Gaussian decay. Part (c) does not contain calculation including internuclear couplings, since direct diagonalization of the corresponding Hamiltonian was not possible with the available computational resources.

magnetic fields. By 'strong coupling' we mean here that the characteristic energy scale of qubit-nucleus coupling (more precisely, of the part of the coupling that leads to qubit-dependent dynamics) is larger than the characteristic energy scale of Hamiltonian of the nucleus, i.e. $A_k^{\perp} \gg \omega$. Only in this limit, in which the qubit-environment coupling $\hat{V}_m$ dominates over the environmental Hamiltonian, $\hat{H}_{\mathrm{E}}$ (a condition known as the 'quantum measurement limit' of decoherence, see [65]), we can expect the qubit to leave a significant trace of its state (or even presence) on the state of the environment.

When looking at statistics of hyperfine couplings for each of a hundred realizations of nuclear bath around NV center, as discussed in appendix C, it becomes clear why $\mu N \approx 20$ corresponds to the formation

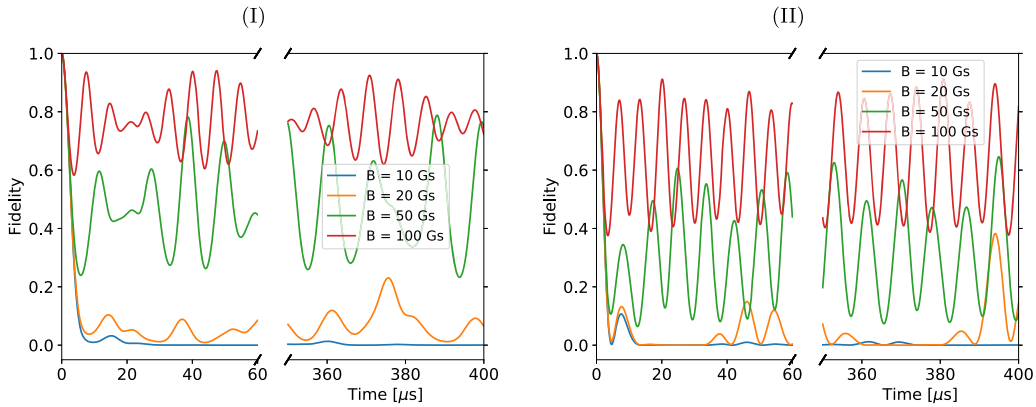

Figure 6. Fidelity for two spatial realizations of the nuclear environment. We assume macrofractions of 20 completely polarized spins ($p = 1$). Each curve corresponds to a different value of external magnetic field (in Gauss), as indicated in the legend. Panels (a) and (b) represent the fidelity on the short and the long timescales respectively.

of SBS: around 15–20 nuclear spins closest to the NV center have the transverse hyperfine exceeding nuclear Zeeman splitting for $B = 10$ G. Additionally, for roughly a half of these spins also the component of the hyperfine coupling parallel to the magnetic field exceeds the Zeeman splittings. For these spins one cannot of course use the weak-coupling approximation, and one has to consider the full form of equations (26) and (28) for fidelity. For a few strongly coupled nuclei, oscillations of fidelity with frequencies $\Omega_k \approx \sqrt{(A_k^{\perp})^2 + (A_k^z)^2}$ should be indeed visible.

5. Conclusions

We have analyzed a realistic model of NV center as a 'simulator' for an important process of the quantum-to-classical transition—the appearance of objectivity. The latter is described by SBS—specific multipartite quantum states, encoding an operational notion of objectivity and related to the idea of quantum Darwinism. From our theoretical analysis it follows that using current state of the art dynamical polarization technique, the post decoherence quantum state of the NV center and two macrofractions, each consisting of about 10 strongly polarized nuclei localized close to the center, comes reasonably close to an SBS form, provided that we keep the external magnetic field below ≈ 20 G, so that the polarized nuclei close to the NV center are strongly coupled to it, i.e. the energy scale of their coupling to the qubit exceeds their Zeeman energy. In these conditions, during the decoherence process the information about the state of the NV center qubit becomes redundantly encoded in its nearest environment in the strongest possible form, and hence becomes objective.

This is, to the best of our knowledge, the first study of SBS using a model that closely describes a system that is actually a subject of ongoing experiments. Let us discuss the possibilities of an experimental verification of our results.

NV center is the only qubit in the considered system that can be directly read out. It is possible to create a coherent quantum state of nuclear spins or even an entangled state of NV center and a few nuclei [61], but then the tomography of such state is performed using NV center coherence. Therefore, a direct observation of an SBS state or measurement of fidelity between conditional states of observed fraction is not possible in a setup with a single NV center qubit, since the state comes into being as a result of central qubit decoherence. However, according to [61], tomography of conditional states of the bath or at least identification of timescales for orthogonalization of conditional states of the observed bath as discussed in this work should be experimentally viable. There, the authors show that it is possible to perform a full state tomography of 8 qubits: the NV center, the nitrogen spin on the defect, and six carbon spins. This can be done by measuring the electron spin in the pointer state basis and conditioned on the measured state of the qubit, application of sequence of rotations both to the carbon and electron spins, intertwined with dynamical decoupling sequence (cf figure 7 in [61]), such that a certain multi-qubit density matrix element can be read out by measurement of the electron spin coherence. Alternatively, one could take advantage of the ability of the NV center qubit to characterize nearby nuclear spins in a two-qubit setup, in which the second qubit is kept in $m = 0$ state (decoupled from the environment) while the first one decoheres, and only after time at which creation of SBS is expected, it is rotated into a superposition state, and its dephasing under dynamical decoupling is used to characterize the state of the nuclear environment

common to the two qubits. In order for polarized spins close to the first qubit to be within such a common environment, the distance between the centers should be a few nanometers [14], which will be challenging to achieve, but it's not inconceivable, with entanglement of two centers separated by ≈ 20 nm achieved a few years ago [66].

Acknowledgments

We acknowledge the financial support by Polish National Science Center (NCN), Grant No. 2015/19/B/ST3/03152 (ŁC), Grant No. 2019/35/B/ST2/01896 (JKK), and PhD Student Scholarship No. 2018/28/T/ST3/00390 (DK). The Publication is financed by the Polish National Agency for Academic Exchange under the Foreign Promotion Programme.

Data availability statement

The data generated and/or analyzed during the current study are not publicly available for legal/ethical reasons but are available from the corresponding author on reasonable request.

Appendix A. Decoherence of a qubit defined between states m and m' due to free evolution with a non-interacting bath

Coherence of a qubit defined between m and m' states evolving freely with a bath of non-interacting spins (from the unobserved part of the environment), in a rotating frame with respect to free Hamiltonian of the qubit, can be expressed as:

$$\gamma_{mm'}(t) = \prod_{k\in(1-\mu)E} \gamma^k_{mm'}(t), \tag{A.1}$$

with the contribution from a single spin k:

$$\begin{aligned}\gamma^k_{mm'}(t) = \cos\frac{\omega_m t}{2}\cos\frac{\omega_{m'}t}{2} + \frac{mm'(A^\perp_k)^2 + (A^z_k m + \omega_k)(A^z_k m' + \omega_k)}{\omega_m\omega_{m'}}\sin\frac{\omega_m t}{2}\sin\frac{\omega_{m'}t}{2}\\ - \mathrm{i}p_k\left(\frac{A^z_k m + \omega_k}{\omega_m}\cos\frac{\omega_{m'}t}{2}\sin\frac{\omega_m t}{2} - \frac{A^z_k m' + \omega_k}{\omega_{m'}}\cos\frac{\omega_m t}{2}\sin\frac{\omega_{m'}t}{2}\right)\end{aligned} \tag{A.2}$$

Appendix B. Fidelity between environmental states conditioned on qubit defined between states m and m'

For a qubit defined between arbitrary m and m' states, fidelity for noninteracting bath can be expressed as stated in equation (27):

$$\mathcal{F}^{\mu E}_{mm'}(t) \equiv \mathcal{F}(\hat\rho^{\mu E}_m(t), \hat\rho^{\mu E}_{m'}(t)) = \prod_{k\in\mu N}\mathcal{F}(\hat\rho^{\mathrm{k}}_m(t), \hat\rho^k_{m'}(t)). \tag{B.1}$$

Contribution for a single member of such macrofraction corresponds to the following formula:

$$\begin{aligned}\mathcal{F}(\hat\rho^{\mathrm{k}}_m(t), \hat\rho^k_{m'}(t)) = 1 + p_k^2\Bigg[(A^\perp_k)^2\left(\frac{m^2}{\omega^2_{\mathrm{m}}}\sin^2\frac{\omega_m t}{2} - \frac{m'^2}{\omega^2_{m'}}\sin^2\frac{\omega_{m'}t}{2}\right)\\ + 2mm'\left(\frac{(A^\perp_k)^2(mA^z_k + \omega_k)(m'A^z_k + \omega_k)}{\omega^2_m\omega^2_{m'}}\sin\frac{\omega_m t}{2}\sin\frac{\omega_{m'}t}{2}\right.\\ \left. + \frac{(A^\perp_k)^2}{\omega_m\omega_{m'}}\sin\omega_m t\sin\omega_{m'}t\right) + \frac{2m^2m'^2(A^\perp_k)^4}{\omega^2_m\omega^2_{m'}}\sin^2\frac{\omega_m t}{2}\sin^2\frac{\omega_{m'}t}{2}\Bigg].\end{aligned} \tag{B.2}$$

From the form of this expression one can observe that equation (28), which corresponds to the case when qubit defined between $m = 0$ and $m' = 1$, simply reduces the above equation to one term proportional to $m^2 = 1$. For a qubit defined between $m = -1$ and $m' = 1$, one needs to consider a complete expression.

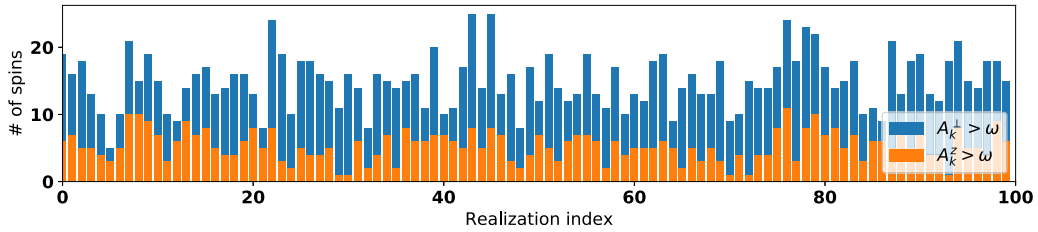

Figure C1. Number of nuclear spins for which transverse or parallel hyperfine interaction value is larger than nuclear Zeeman splitting for $B = 10$ G, where $A_k^\perp$ corresponds to the perpendicular and A_k^z to the parallel coupling of kth nuclear spin to the NV center, and ω is the Zeeman splitting (equal for all nuclear spins in a constant magnetic field).

Appendix C. Fidelity for very strongly coupled nuclear spins

In the limit of very strong coupling to the qubit, i.e. when $A_k^z \gg \omega_k$ and $t \ll \frac{1}{\omega_k}\sqrt{1+\frac{(A_k^\perp)^2}{(A_k^z)^2}}$, this formula becomes:

$$\mathcal{F}^{\mu E}(t) \approx \prod_{k\in\mu N}\left[1 - p_k^2\frac{(A_k^\perp)^2}{|A_k|^2}\left(1-\frac{2\omega A_k^z}{|A_k|^2}\right)\sin^2\left(\frac{t}{2}|A_k|\right)\right], \tag{C.1}$$

where $|A_k| = \sqrt{(A_k^\perp)^2 + (A_k^z)^2}$. This limit can either correspond to strong oscillations observable on the timescale of orthogonalization of qubit-conditional states of a given macrofraction or, when exceeding a certain number of such spins, a rapid decay of fidelity as a function of total evolution time.

When looking at statistics of hyperfine couplings for each of a hundred realizations of nuclear bath around NV center, as represented in the figure C1 it becomes clear why $N \approx 20$ corresponds to formation of SBS, as around 15–20 nuclear spins closest to the NV center should have transverse hyperfine couplings which exceed nuclear Zeeman splitting for $B = 10$ G. Additionally, for roughly a half of these spins also component of the hyperfine coupling parallel to the magnetic field exceeds the Zeeman splittings. For these spins it is not practical to discuss the relevance of weakly coupled bath, however one should expect that the oscillations observed in fidelity for high magnetic fields, corresponds to dynamics of a few nuclear spins.

ORCID iDs

Damian Kwiatkowski https://orcid.org/0000-0003-1013-286X
Łukasz Cywiński https://orcid.org/0000-0002-0162-7943
Jarosław K. Korbicz https://orcid.org/0000-0003-2084-7906

References

[1] Zurek W H 1982 *Phys. Rev.* D **26** 1862–80
[2] Cucchietti F M, Paz J P and Żurek W H 2005 *Phys. Rev.* A **72** 052113
[3] Hanson R, Kouwenhoven L P, Petta J R, Tarucha S and Vandersypen L M K 2007 *Rev. Mod. Phys.* **79** 1217
[4] Coish W A and Baugh J 2009 *Phys. Status Solidi* B **246** 2203
[5] Cywiński Ł 2011 *Acta Phys. Pol.* A **119** 576
[6] Urbaszek B, Marie X, Amand T, Krebs O, Voisin P, Maletinsky P, Högele A and Imamoglu A 2013 *Rev. Mod. Phys.* **85** 79
[7] Chekhovich E A, Makhonin M N, Tartakovskii A I, Yacoby A, Bluhm H, Nowack K C and Vandersypen L M K 2013 *Nat. Mater.* **12** 494
[8] Yang W, Ma W-L and Liu R-B 2017 *Rep. Prog. Phys.* **80** 016001
[9] Dobrovitski V V, Fuchs G D, Falk A L, Santori C and Awschalom D D 2013 *Annu. Rev. Condens. Matter Phys.* **4** 23
[10] Rondin L, Tetienne J-P, Hingant T, Roch J-F, Maletinsky P and Jacques V 2014 *Rep. Prog. Phys.* **77** 056503
[11] Zhao N, Wang Z Y and Liu R B 2011 *Phys. Rev. Lett.* **106** 217205
[12] Roszak K and Korbicz J K 2019 *Phys. Rev.* A **100** 062127
[13] Zhao N *et al* 2012 *Nat. Nanotechnol.* **7** 657–62
[14] Kwiatkowski D and Cywiński L 2018 *Phys. Rev.* B **98** 155202
[15] Staudacher T, Shi F, Pezzagna S, Meijer J, Du J, Meriles C A, Reinhard F and Wrachtrup J 2013 *Science* **339** 561
[16] Lovchinsky I *et al* 2016 *Science* **351** 836
[17] Degen C L, Reinhard F and Cappellaro P 2017 *Rev. Mod. Phys.* **89** 035002
[18] Zhao N, Ho S W and Liu R B 2012 *Phys. Rev.* B **85** 115303
[19] Le T P and Olaya-Castro A 2020 *Quantum Sci. Technol.* **5** 045012
[20] Lorenzo S, Paternostro M and Palma G M 2020 *Phys. Rev. Res.* **2** 013164
[21] García-Pérez G, Chisholm D A, Rossi M A C, Palma G M and Maniscalco S 2020 *Phys. Rev. Res.* **2** 012061

[22] Balaneskovic N 2015 *Eur. Phys. J.* D **69** 232
[23] Zwolak M, Quan H T and Zurek W H 2009 *Phys. Rev. Lett.* **103** 110402
[24] Fuchs C A and van de Graaf J 1999 *IEEE Trans. Inf. Theor.* **45** 1216
[25] Oliveira S M, de Paula A L and Drumond R C 2019 *Phys. Rev.* A **100** 052110
[26] Unden T K, Louzon D, Zwolak M, Zurek W H and Jelezko F 2019 *Phys. Rev. Lett.* **123** 140402
[27] Chen M-C, Zhong H-S, Li Y, Wu D, Wang X-L, Li L, Liu N-L, Lu C-Y and Pan J-W 2019 *Sci. Bull.* **64** 580
[28] Ciampini M A, Pinna G, Mataloni P and Paternostro M 2018 *Phys. Rev.* A **98** 020101
[29] Ollivier H, Poulin D and Zurek W H 2004 *Phys. Rev. Lett.* **93** 220401
[30] Zurek W H 2009 *Nat. Phys.* **5** 181
[31] Korbicz J K, Horodecki P and Horodecki R 2014 *Phys. Rev. Lett.* **112** 120402
[32] Horodecki R, Korbicz J K and Horodecki P 2015 *Phys. Rev.* A **91** 032122
[33] Ryan EPaternostro M and Campbell S 2020 arXiv:2011.13385
[34] Giorgi G L, Galve F and Zambrini R 2015 *Phys. Rev.* A **92** 022105
[35] Tuziemski J and Korbicz J K 2015 *Europhys. Lett.* **112** 40008
[36] Mironowicz P, Korbicz J K and Horodecki P 2017 *Phys. Rev. Lett.* **118** 150501
[37] Korbicz J K, Aguilar E A, Ćwikliński P and Horodecki P 2017 *Phys. Rev.* A **96** 032124
[38] Scandolo C M, Salazar R, Korbicz J K and Horodecki P 2018 arXiv:1805.12126
[39] Tuziemski J, Lampo A, Lewenstein M and Korbicz J K 2019 *Phys. Rev.* A **99** 022122
[40] Le T P and Olaya-Castro A 2019 *Phys. Rev. Lett.* **122** 010403
[41] Le T P and Olaya-Castro A 2018 *Phys. Rev.* A **98** 032103
[42] Korbicz J K 2020 arXiv:2007.04276
[43] Zurek W H 1981 *Phys. Rev.* D **24** 1516–25
[44] Roszak K and Korbicz J K 2019 *Phys. Rev.* A **100** 062127
[45] London P *et al* 2013 *Phys. Rev. Lett.* **111** 067601
[46] Fischer R, Bretschneider C O, London P, Budker D, Gershoni D and Frydman L 2013 *Phys. Rev. Lett.* **111** 057601
[47] Fischer R, Jarmola A, Kehayias P and Budker D 2013 *Phys. Rev.* B **87** 125207
[48] Pagliero D *et al* 2018 *Phys. Rev.* B **97** 024422
[49] Wunderlich R, Kohlrautz J, Abel B, Haase J and Meijer J 2017 *Phys. Rev.* B **96** 220407
[50] Álvarez G A, Bretschneider C O, Fischer R, London P, Kanda H, Onoda S, Isoya J, Gershoni D and Frydman L 2015 *Nat. Commun.* **6** 8456
[51] King J P, Jeong K, Vassiliou C C, Shin C S, Page R H, Avalos C E, Wang H J and Pines A 2015 *Nat. Commun.* **6** 8965
[52] Scheuer J, Schwartz I, Müller S, Chen Q, Dhand I, Plenio M B, Naydenov B and Jelezko F 2017 *Phys. Rev.* B **96** 174436
[53] Hovav Y, Naydenov B, Jelezko F and Bar-Gill N 2018 *Phys. Rev. Lett.* **120** 060405
[54] Schwartz I *et al* 2018 *Sci. Adv.* **4** eaat8978
[55] Mironowicz P, Należyty P, Horodecki P and Korbicz J K 2018 *Phys. Rev.* A **98** 022124
[56] Gali A, Fyta M and Kaxiras E 2008 *Phys. Rev.* B **77** 155206
[57] Roszak K and Cywiński Ł 2015 *Phys. Rev.* A **92** 032310
[58] Liu G Q, Pan X Y, Jiang Z F, Zhao N and Liu R B 2012 *Sci. Rep.* **2** 432
[59] Roszak K and Cywiński L 2018 *Phys. Rev.* A **97** 012306
[60] Zhao N, Hu J-L, Ho S-W, Wan J T K and Liu R B 2011 *Nat. Nanotechnol.* **6** 242
[61] Bradley C E, Randall J, Abobeih M H, Berrevoets R C, Degen M J, Bakker M A, Markham M, Twitchen D J and Taminiau T H 2019 *Phys. Rev.* X **9** 031045
[62] Abobeih M H, Randall J, Bradley C E, Bartling H P, Bakker M A, Degen M J, Markham M, Twitchen D J and Taminiau T H 2019 *Nature* **576** 411–5
[63] Yang W and Liu R B 2008 *Phys. Rev.* B **78** 085315
[64] Yang W and Liu R B 2009 *Phys. Rev.* B **79** 115320
[65] Schlosshauer M 2007 *Decoherence* (*and the Quantum-To-Classical Transition*) (Berlin: Springer)
[66] Dolde F *et al* 2013 *Nat. Phys.* **9** 139